Prendergast, N. J., Delcamp, T. J., Smith, P. L., & Freisheim, J. H. (1988) *Biochemistry 27*, 3664-3671.
Ratnam, J., Tan, X., Prendergast, N. J., Smith, P., & Freisheim, J. H. (1988) *Biochemistry 27*, 4800-4804.
Sanger, F., Nicklen, S., & Coulson, A. (1977) *Proc. Natl. Acad. Sci. U.S.A. 74*, 5463-5467.
Seeger, D. R., Cosulich, D. B., Smith, J. M., & Hultquist, M. E. (1949) *J. Am. Chem. Soc. 71*, 1753.
Stone, S. R., & Morrison, J. F. (1984) *Biochemistry 23*, 2753-2758.
Teale, F. W. J. (1960) *Biochem. J. 76*, 381-388.
Teale, F. W. J., & Weber, G. (1957) *Biochem. J. 65*, 476-482.
Vesterberg, O. (1971) *Methods Enzymol. 22*, 389-412.
Volz, K. W., Matthews, D. A., Alden, R. A., Freer, S. T., Hamsch, G., Kaufman, B. T., & Kraut, J. (1982) *J. Biol. Chem. 257*, 2528-2536.
Warwick, P. E., D'Souza, L., & Freisheim, J. H. (1972) *Biochemistry 11*, 3775-3779.
Westhof, E. D., Altschub, D., Moras, D., Bloomer, A. C., Mondragon, A., Klug, A., & Van Regenmortel, A. (1984) *Nature (London) 311*, 123-126.
Williams, J. W., & Morrison, J. F. (1981) *Biochemistry 20*, 6024-6029.
Williams, J. W., Morrison, J. F., & Duggleby, R. G. (1979) *Biochemistry 18*, 2567-2573.
Williams, M. N. (1975) *J. Biol. Chem. 250*, 322-330.
Yanisch-Perron, C., Vieiva, J., & Messing, J. (1985) *Gene 33*, 103-119.

Probing the Functional Role of Threonine-113 of *Escherichia coli* Dihydrofolate Reductase for Its Effect on Turnover Efficiency, Catalysis, and Binding†

C. A. Fierke‡ and S. J. Benkovic*,§

Biochemistry Department, Box 3711, Duke University Medical Center, Durham, North Carolina 27710, and Department of Chemistry, 152 Davey Laboratory, The Pennsylvania State University, University Park, Pennsylvania 16802

Received June 21, 1988; Revised Manuscript Received August 30, 1988

ABSTRACT: The role of Thr-113 of *Escherichia coli* dihydrofolate reductase in binding and catalysis was probed by amino acid substitution. Thr-113, a strictly conserved residue that forms a hydrogen bond to the active-site Asp-27 and to the amino group of methotrexate through a fixed water molecule, was replaced by valine. The kinetic scheme is identical in form with the wild-type scheme, although many of the rate constants vary, including a decrease in the association rate constants and an increase in the dissociation rate constants for folate ligands, a decrease in the hydride-transfer rate constant in both directions, and an increase in the intrinsic pK_a of Asp-27. Overall, replacement of Thr-113 by Val decreases the binding of folate substrates by ≈2.3 kcal/mol. These multiple complex changes on various ground and transition states underscore the optimal properties of a strictly conserved residue in the evolution of catalytic function.

Dihydrofolate reductase (5,6,7,8-tetrahydrofolate:NADP oxidoreductase, EC 1.5.1.3) catalyzes the NADPH-dependent reduction of 7,8-dihydrofolate (H_2F)[1] to 5,6,7,8-tetrahydrofolate (H_4F). This enzyme is necessary for maintaining intracellular pools of H_4F and its derivatives, which are essential cofactors in the one-carbon-transfer reactions utilized in the biosynthesis of purines, thymidylate, and several amino acids. In addition it is the target enzyme of a group of antifolate drugs that are widely used as antitumor and antimicrobial agents such as methotrexate (MTX), trimethoprim (TMP), and pyrimethamine. Because of its biological and pharmacological importance, dihydrofolate reductase (DHFR) has been the subject of intensive structural and kinetic studies. The structures of the *Escherichia coli*, *Lactobacillus casei*, and chicken liver enzymes have been determined to 1.7-Å resolution for some binary and ternary complexes (Bolin et al., 1982; Filman et al., 1982; Matthews et al., 1985). In addition, a complete kinetic scheme for wild-type DHFR has been derived from pre-steady-state and steady-state kinetics (Fierke et al., 1987a). Despite knowledge of the kinetics and the identities of the amino acids at the active site of DHFR, the function of the amino acids in binding and catalysis is unclear. We have utilized site-directed mutagenesis combined with detailed kinetic analysis to establish structure–function relationships for *E. coli* DHFR.

Site-directed mutagenesis is a powerful tool that has been used to elucidate the functional role of individual amino acids in DHFR (Villafranca et al., 1983, 1987; Chen et al., 1985, 1987; Howell et al., 1985, 1987; Mayer et al., 1986; Taira et al., 1987a; Taira & Benkovic, 1988; Benkovic et al., 1988). The substrate H_2F, binds tightly to dihydrofolate reductase in a conformation with the pteridine ring nearly perpendicular to the *p*-aminobenzoyl group (Bolin et al., 1982; Filman et al., 1982). The binding site is lined with several strictly conserved amino acids. One of these, Thr-113, forms one hydrogen bond with Asp-27, the proton-donating residue (Howell et al., 1985), and another with the amino group of methotrexate (and presumably H_2F) indirectly through a bound water molecule. In this work we investigate the importance of these hydrogen

† This work was supported in part by NIH Grant GM24129. C.A.F. is the recipient of a National Institutes of Health postdoctoral fellowship (GM10072).
‡ Duke University Medical Center.
§ The Pennsylvania State University.

[1] Abbreviations: H_2F, 7,8-dihydrofolate; H_4F, 5,6,7,8-tetrahydrofolate; DHFR, dihydrofolate reductase; MTX, methotrexate; TMP, trimethoprim; NADPH, NH, reduced nicotinamide adenine dinucleotide phosphate; NADP, N, nicotinamide adenine dinucleotide phosphate; DAM, 2,4-diamino-6,7-dimethylpteridine; Fol, folate.

0006-2960/89/0428-0478$01.50/0

bonds for binding and catalysis by determining the complete kinetic scheme for the Thr-113 → Val mutation (Chen et al., 1985). We then evaluate the wild-type and mutant kinetic schemes in terms of their overall efficiency under physiological conditions.

Materials and Methods

Materials

7,8-Dihydrofolate (H_2F) was prepared from folic acid by the method of Blakley (1960), and (6*S*)-tetrahydrofolate (H_4F) was prepared from H_2F by using dihydrofolate reductase (Mathews & Huennekens, 1960) and purified on DE-52 resin eluting with a triethylammonium bicarbonate linear gradient (Curthoys et al., 1972). NADPH, NADP, trimethoprim (TMP), methotrexate (MTX), and folic acid were purchased from Sigma Chemical Co. 2,4-Diamino-6,7-dimethylpteridine (DAM) was purchased from ICN Pharmaceuticals. [4′(*R*)-^{2}H]NADPH was prepared (Stone & Morrison, 1982) by using *Leuconostoc mesenteroides* alcohol dehydrogenase obtained from Research Plus, Inc., and purified by the method of Viola et al. (1979). The concentrations of the ligands were determined spectrophotometrically by using the following extinction coefficients: H_2F, 28 000 M^{-1} cm^{-1} at 282 nm, pH 7.4 (Dawson et al., 1969); H_4F, 28 000 M^{-1} cm^{-1} at 297 nm, pH 7.5 (Kallen & Jencks, 1966); folic acid, 27 600 M^{-1} cm^{-1} at 282 nm, pH 7.0 (Rabinowitz, 1960); TMP, 6060 M^{-1} cm^{-1} at 271 nm in 0.1 M acetic acid (Roth & Strelitz, 1969); MTX, 22 100 M^{-1} cm^{-1} at 302 nm in 0.1 M KOH (Seeger et al., 1949); DAM, 6900 M^{-1} cm^{-1} at 346 nm, pH 6.0 (Brown & Jacobsen, 1961); NADPH, 6200 M^{-1} cm^{-1} at 339 nm, pH 7.5; and NADP, 18 000 M^{-1} cm^{-1} at 259 nm, pH 7.0 (P-L Biochemicals, 1961). The concentration of H_4F was also determined enzymatically by using a molar absorbancy change for the 10-formyl-H_4F synthetase reaction of 12 000 M^{-1} cm^{-1} at 312 nm (Smith et al., 1981). The concentration of H_2F or NADPH was also determined enzymatically by using a molar absorbancy change for the dihydrofolate reductase reaction of 11 800 M^{-1} cm^{-1} at 340 nm (Stone & Morrison, 1982).

The Val-113 mutant was constructed by Ruth Mayer, as previously described (Chen et al., 1985), by primer extension of oligonucleotides (Smith, 1985) using as the template partially single-stranded plasmid DNA in which a 1-kb fragment containing the DHFR (*fol*) gene (Smith & Calvo, 1980) was inserted into the *Bam*H1 site of a 4.4-kb pBR322 derivative plasmid lacking the *Eco*R1 site (Taira et al., 1987a). Val-113 DHFR was purified from an *E. coli* mutant strain SF32 (Singer et al., 1985), transformed with the *fol* plasmid encoding the Val-113 mutant DHFR. The SF32 strain, a generous gift from Sara Singer, is a mutant *E. coli* strain containing a *rec*A*56* allele and apparently devoid of DHFR activity (*fol-200*). This strain was used to prevent contamination of the mutant (Val-113) protein preparations with chromosomal wild-type DHFR. Purification was carried out by using a methotrexate affinity resin method described by Baccanari et al. (1977). The concentration of purified DHFR was determined by methotrexate titration (Williams et al., 1979).

Methods

All measurements were performed at 25 °C in a buffer containing 50 mM 2-(*N*-morpholino)ethanesulfonic acid, 25 mM tris(hydroxymethyl)aminomethane, 25 mM ethanolamine, 100 mM sodium chloride, 1 mM ethylenediaminetetraacetate, and 1 mM dithioerythritol (MTEN buffer). Over the pH range used, the ionic strength of this buffer remains constant (Ellis & Morrison, 1982). Additionally, in some cases the buffer was purged with argon, which had no observable effect on the kinetics.

Steady-State Kinetics. Initial velocities for dihydrofolate reductase reactions were determined by measuring the rate of either the enzyme-dependent decrease in H_2F and NADPH or, in the reverse direction, the increase in H_2F and NADPH at 340 nm (Fierke et al., 1987) using a molar absorbancy change of 11 800 M^{-1} cm^{-1} (Stone & Morrison, 1982). DHFR was preincubated with NADPH or NADP before turnover was initiated to remove hysteretic behavior (Penner & Frieden, 1985). The inhibition constant of DAM, $K_{i,obs}$ (the observed dissociation constant of DAM from the E·NADPH·DAM complex), was obtained by plotting $1/v$ versus the inhibitor concentration (Segel, 1975). These data were fit by using the program RS1 run on a Micro-Vax. $K_{i,app}$ was calculated from $K_{i,obs}$ as

$$K_{i,app} = K_{i,obs}/(1 + [H_2F]/K_M) \quad (1)$$

Transient Kinetics. Binding and pre-steady-state kinetics were obtained by using a stopped-flow apparatus, operating in either a fluorescence or transmittance mode, built in the laboratory of Johnson (1986) that has a 1.6-ms dead time, a 2-mm sample cell, and a thermostated sample cell. Interference filters (Corion Corp.) were used on both the light input (excitation) and output (emission). In most cases the formation of an enzyme–substrate complex was followed by using a 290-nm interference filter on the excitation input and then monitoring either the quenching of the intrinsic enzyme fluorescence with an output filter at the emission wavelength of 340 nm or the enhancement of coenzyme fluorescence with an output filter of 450 nm (Lackowicz, 1983; Velick, 1958; Dunn & King, 1980). Transmittance measurements were made by using a 340-nm input filter and were later converted to absorbance. A molar absorbancy change for this reaction of 8500 M^{-1} cm^{-1} using the 340-nm bandpass filter was determined at low enzyme concentration (Fierke et al., 1987a). For slow reactions a neutral density filter (0.2–2.0 OD) was placed on the input to decrease the light intensity and thus decrease photobleaching of the sample. In most experiments the average of at least four runs was used for data analysis.

Data were collected by a computer over a given time interval following a trigger impulse. All data were analyzed by an iterative, nonlinear least-squares fit computer program using a modification of the method of moments (Dyson & Isenberg, 1971; Johnson, 1986). Kinetic data were analyzed with either a single exponential, a double exponential, or a single exponential followed by a linear rate. The data were then transferred to a Vax microcomputer where a fit to more complicated models was tested by using the computer program KINSIM (Barshop et al., 1983). This latter method was used to estimate the rate constant for hydride transfer at various pH's.

Fluorescence Titrations. Thermodynamic dissociation constants (K_Ds) were determined by fluorescence titration whereby the formation of the E·L complex was followed by measuring the quenching of the tryptophan fluorescence of the enzyme upon addition of ligand using an excitation wavelength of 290 nm together with an emission wavelength of 340 nm (Birdsall et al., 1980; Morrison & Stone, 1982; Taira & Benkovic, 1988). For MTX titration the enzyme concentration employed was 2.5 nM ($>K_D$) with the excitation and emission slits set at 8 and 16 nm, respectively, to maximize the signal. A solution of tryptophan was used to determine the correction factor for the inner filter effect. The data were fit to eq 2, where E_T is the enzyme concentration, F_E is the initial fluorescence, F_{EL} is the final fluorescence, and L_T is the total ligand concentration, by use of a nonlinear least-squares

Scheme I

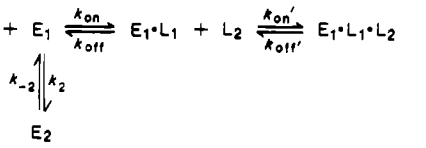

Table I: Kinetic Binding Constants: Relaxation Method

ligand	enzyme species	$10^{-6}k_{on}$ (M^{-1} s^{-1}) Val-113	$10^{-6}k_{on}$ (M^{-1} s^{-1}) wild-type	k_{off} (s^{-1}) Val-113	k_{off} (s^{-1}) wild-type
H_2F	E	3 ± 1	42 ± 2[a]	175 ± 25	47 ± 10[a]
H_4F	E	6 ± 1	24 ± 1[a]	29 ± 10	≤1[a]
	E·NH	0.56 ± 0.05	2.3 ± 0.2[a]	66 ± 4	10 ± 3[a]
DAM	E	3.4 ± 1	12 ± 1[b]	95 ± 20	35 ± 5[b]
NH	E	22 ± 1	20 ± 1[a]	14 ± 5	3.5 ± 1.5[a]
	E·H_4F	1.6 ± 0.2	8 ± 0.3[a]	63 ± 5	85 ± 20[a]
N	E	4 ± 1	13 ± 3[a]	225 ± 15	295 ± 25[a]

[a] Taken from Fierke et al. (1987a). [b] Taken from Taira and Benkovic (1988).

fitting program, NLIN (Marquardt method) (Taira & Benkovic, 1988).

$$F = F_E - C(F_E - F_{EL})/2E_T \quad (2)$$

where

$$C = 2[E\cdot L] = (E_T + L_T + K_D) - [(E_T + L_T + K_D)^2 - 4(E_T)(L_T)]^{1/2}$$

RESULTS

Binding Kinetics—Relaxation Method. The rate constant for binding ligands to DHFR in either the cofactor or the folate binding site can be measured by following the quenching of the intrinsic enzyme fluorescence. In the formation of binary complexes of DHFR at saturating substrate concentration, two exponentials were observed: a rapid, ligand-dependent phase followed by a ligand-independent phase (Dunn et al., 1978; Dunn & King, 1980; Cayley et al., 1981). Similar behavior is observed for binding NADPH to either wild-type DHFR or Val-113 mutant DHFR; the ratio of the amplitude of the fast phase compared to the slow phase is 0.72 ± 0.09 or 1.2 ± 0.1 for wild-type and Val-113, respectively, and the rate constant for the ligand-independent slow phase is 0.034 ± 0.005 or 0.05 ± 0.006 s^{-1}, respectively. In the formation of ternary complexes a single ligand-dependent exponential is observed as described by previous studies (Dunn et al., 1978; Dunn & King, 1980; Cayley et al., 1981). Cayley et al. (1981) concluded that this behavior is due to the mechanism shown in Scheme I, where substrate binds rapidly to only one of two enzyme conformers (at these substrate levels) and interconversion between the conformers is slow.

In the ligand-dependent reactions the observed first-order rate constants increased linearly with the ligand concentration, showing no sign of saturation. For a simple association reaction, the observed rate constant under pseudo-first-order conditions may be approximated by $k_{obs} = k_{on}[L] + k_{off}$, where k_{on} and k_{off} are the association and dissociation rate constants, respectively. Thus, in a linear plot of k_{obs} vs [L] the slope is k_{on} and the intercept is k_{off}. Assuming a simple association reaction for the ligand-dependent phase, the association and dissociation rate constants for binding H_2F, H_4F, NADPH, and NADP to both free enzyme and a variety of binary complexes were measured at pH 6 in MTEN buffer, 25 °C, and the results for Val-113 and wild-type DHFR are displayed in Table I.

Competition Experiments. The dissociation rate constant of a ligand from the DHFR–ligand complex can be measured by a competition experiment (Birdsall et al., 1980). In this technique the enzyme–ligand complex ($E\cdot L_1$) is mixed with a large excess of a second ligand that competes for the binding site (see Scheme II), and the formation of the new enzyme–ligand complex ($E\cdot L_2$) is monitored by a fluorescence change due to the difference in fluorescence quenching by the two ligands. When $k_1[L_1] \ll k_2[L_2] \gg k_{-1}$, the fluorescence change is attributable to the conversion of $E\cdot L_1$ to $E\cdot L_2$ characterized by a single-exponential decay determined by the dissociation rate constant for L_1, k_{-1}. The validity of these conditions is checked by showing that k_{obs} is independent of the concentration of both L_1 and L_2. Dissociation rate constants determined with this technique for both wild-type and Val-113 DHFR for a variety of ligands in MTEN buffer, pH 6, 25 °C, are shown in Table II.

Table II: Dissociation Rate Constants: Competition Method

ligand[a]	enzyme species[a]	trapping ligand[a]	k_{off} (s^{-1}) Val-113	k_{off} (s^{-1}) wild-type
H_2F	E·H_2F	TMP	195 ± 35	22 ± 5[b]
H_4F	E·H_4F	MTX, TMP	38 ± 3	1.4 ± 0.2[b]
	E·N·H_4F	MTX, TMP	34 ± 6	2.4 ± 0.2[b]
	E·NH·H_4F	MTX, TMP	70 ± 15	12 ± 2[b]
DAM	E·DAM	MTX, TMP	120 ± 5	24 ± 1[c]
NH	E·NH	N	21 ± 3	3.6 ± 0.5[b]
	E·H_4F·NH	N	60 ± 4	85 ± 10[b]
	E·Fol·NH	N	3.6 ± 0.2	
N	E·N	NH	230 ± 25	290 ± 20[b]
	E·H_4F·N	NH	185 ± 20	200 ± 20[b]

[a] Abbreviations: H_2F, dihydrofolate; H_4F, tetrahydrofolate; TMP, trimethoprim; MTX, methotrexate; DAM, 2,4-diamino-6,7-dimethylpteridine; N, NADP; NH, NADPH; Fol, folate. [b] Taken from Fierke et al. (1987a). [c] Taken from Taira et al. (1988).

Table III: Comparison of Equilibrium Binding Constants for Wild-Type and Val-113 DHFR at pH 6 and 25 °C in MTEN Buffer

ligand	K_D Val-113	K_D Thr-113	$\Delta\Delta G$ (kcal/mol)
MTX (nM)	0.5 ± 0.1	0.02 ± 0.07[a]	2.3 ± 1.3
H_2F (μM)	≥12 (45 ± 20)[b]	0.22 ± 0.06[c]	>2.3 (3.1 ± 0.5)
H_4F (μM)	4.8 ± 2.4[b]	0.1 ± 0.01[c]	2.3 ± 0.5
NADPH (μM)	1.1 ± 0.2	0.33 ± 0.06[c]	0.71 ± 0.22
NADP (μM)	36 ± 3	24 ± 4	0.2 ± 0.1

[a] Taken from Taira and Benkovic (1988). [b] Calculated from $K_D = k_{off}/k_{on}$. [c] Taken from Fierke et al. (1987a).

Scheme II

$$E\cdot L_1 \underset{k_1}{\overset{k_{-1}}{\rightleftharpoons}} E + L_1$$

$$E + L_2 \underset{k_{-2}}{\overset{k_2}{\rightleftharpoons}} E\cdot L_2$$

Measurements of Thermodynamic Dissociation Constants. The binding of MTX, NADPH, and NADP to DHFR was determined by following the decrease in enzyme fluorescence that occurs upon formation of DHFR–ligand complexes. The data for the resulting fluorescence titration curves were fit to eq 2 in order to calculate the thermodynamic dissociation constants (K_D). Values for K_Ds for Val-113 and wild-type DHFR are listed in Table III. A comparison of the results for the rate and equilibrium constants for H_4F, DAM, NADPH, and NADP shows that the assumption of a simple association step for the ligand-dependent step is reasonable. The dissociation rate constants measured by the two techniques, relaxation and competition experiments, are identical, showing that there are no slow isomerization steps following association. Furthermore, the ratio of k_{off}/k_{on} is similar to the observed K_D measured in the steady state. For H_2F binding to wild-type, the ratio of k_{off}/k_{on} does not correspond

Table IV: Steady-State Parameters for Val-113 and Wild-Type DHFR in MTEN Buffer at 25 °C

	Val-113		wild-type
	predicted	measured	measured
100 μM, NADPH, varying H_2F			
k_{cat} (s^{-1})	35	32.9 ± 0.5	12.3 ± 0.7[a]
pK_a	7.74	7.81 ± 0.15[b]	8.4[c]
$^Hk/^Dk$ (pH 5.5)	1.5	1.54 ± 0.08	1.0 ± 0.1[d]
$^Hk/^Dk$ (pH 9.5)	3.0	3.2 ± 0.2[b]	2.9 ± 0.08[d]
k_{cat}/K_M (M^{-1} s^{-1})	1.9×10^6	$(1.55 \pm 0.07) \times 10^6$	$(1.8 \pm 0.3) \times 10^7$[a]
pK_a	7.36	7.48 ± 0.15[b]	8.1[b]
$^Hk/^Dk$ (pH 5.5)	2.1	2.3 ± 0.4	
$^Hk/^Dk$ (pH 9.5)	3.0	3.0 ± 0.4[b]	3.19 ± 0.22[d]
K_M (μM)	18.4	21.4 ± 1.1	0.7 ± 0.2[a]
180 μM H_4F, 2 mM NADP			
k_{cat} (s^{-1})	0.15	0.14 ± 0.02	0.55 ± 0.1

[a] Data taken from Fierke et al. (1987a). [b] Data taken from Chen et al. (1985) and unpublished data from R. J. Mayer and S. J. Benkovic. [c] Data taken from Stone and Morrison (1984). [d] Data taken from Chen et al. (1987).

Scheme III: pH-Independent Kinetic Scheme for Val-113 Dihydrofolate Reductase in MTEN Buffer, 25 °C[a]

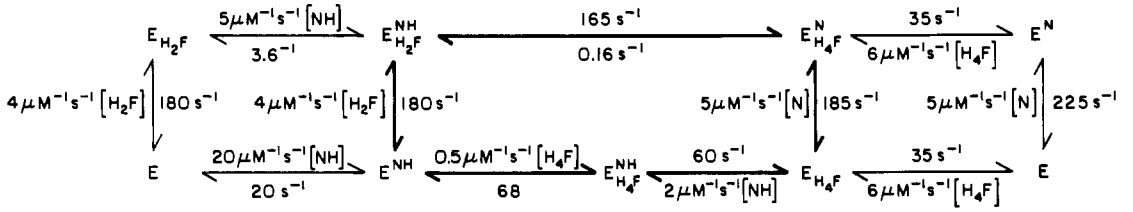

[a] The heavy arrows indicate the kinetic pathway for steady-state turnover at saturation substrate conditions. N, NADP; NH, NADPH; H_2F, dihydrofolate; H_4F, tetrahydrofolate.

to the measured K_D, suggesting that the binding of this ligand may involve either an isomerization step or binding to both E_1 and E_2. The viscosity dependence of association rates for ligand binding to DHFR suggests that these reactions are diffusion-controlled for wild-type (Penner & Frieden, 1987). In the Val-113 mutant the association rate constants for folate ligands have decreased by a factor of 4–10-fold, which suggests that these rate constants are no longer diffusion-limited.

Steady-State Kinetics. The steady-state kinetic parameters for the reaction of Val-113 DHFR with varied H_2F at saturating NADPH (100 μM) were measured at pH 5.5 in MTEN buffer at 25 °C to be k_{cat} = 32.4 ± 0.4 s^{-1}, k_{cat}/K_M = (1.5 ± 0.6) 10^6 M^{-1} s^{-1}, and K_M = 21.4 ± 1.1 μM. Under identical conditions, the observed deuterium kinetic isotope effects, on the steady-state parameters were measured at 100 μM NADPD to be $^D(k_{cat})$ = 1.54 ± 0.08 and $^D(k_{cat}/K_M)$ = 2.3 ± 0.4. The rate of the reverse reaction (net conversion of H_4F and NADP to form H_2F and NADPH) was measured in the steady state from the increase in absorbance at 340 nm. The observed rate was 0.02 ΔOD_{340}/min when Val-113 DHFR (0.397 μM) was added to H_4F (310 μM) and NADP (2.0 mM) in MTEN buffer, pH 10.0, 25 °C. The rate of this reaction was virtually unaffected when the concentration of either substrate was halved or the pH was decreased to 9.0, which implies that this is the pH-independent saturated rate constant for turnover, so k_{cat} = 0.14 ± 0.02 s^{-1}. The steady-state kinetic parameters for Val-113 and wild-type DHFR are summarized in Table IV.

Pre-Steady-State Experiments. The rate constant for hydride transfer from NADPH to H_2F can be determined from the rate constant and amplitude of a burst of product formation measured in pre-steady-state experiments. Val-113 DHFR was preincubated with NADPH or NADPD and diluted 2-fold into H_2F to initiate the reaction, which was monitored by measuring a decrease in absorbance due to disappearance of NADPH(D) and H_2F using a 340-nm bandpass filter, as shown in Figure 1 at pH 6, MTEN buffer, 25 °C. From a comparison of the NADPH and NADPD data it is apparent

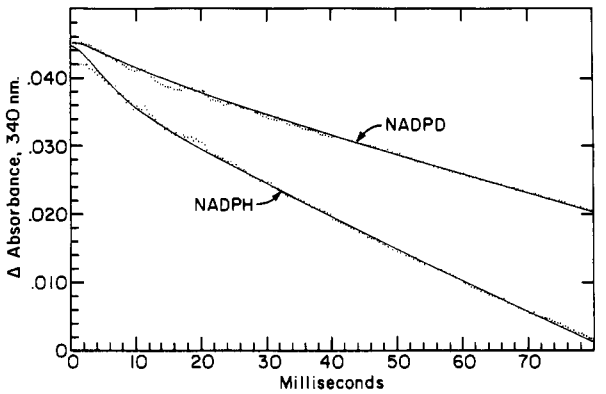

FIGURE 1: Measurement of the pre-steady-state burst by stopped-flow absorbance spectroscopy. DHFR is preincubated with NADPH or [4′(*R*)-^{2}H]NADPD, and the reaction is initiated by addition of H_2F. Final conditions are 9.8 μM Val-113 DHFR, 86.5 μM NADPH (D), and 112 μM H_2F in MTEN buffer, pH 6.0, 25 °C. The solid line is simulated by the computer program KINSIM (Barshop & Frieden, 1983) using the rate constants shown in Scheme III except for $^Hk_{hyd}$ = 155 s^{-1} and $^Dk_{hyd}$ = 49 s^{-1} at pH 6.0.

that there is an isotope effect on both the burst rate constant and the steady-state turnover rate. When these data are fit by the simple model of a single-exponential decay followed by a linear rate, the observed kinetic parameters are k_{burst} = 185 ± 20 s^{-1} (H), 105 ± 30 s^{-1} (D); $amp_{burst}/[E]$ = 0.35 ± 0.06 (H), 0.27 ± 0.06 (D); and k_{cat} = 30.9 ± 1.2 s^{-1} (H), 18.6 ± 1.2 s^{-1} (D). Both the small amplitude and the small isotope effect of 1.7 on the pre-steady-state rate suggest that hydride transfer is not the sole rate-limiting step in the pre-steady-state. The rate constant for hydride transfer was thus estimated by using the computer simulation program KINSIM (Barshop & Frieden, 1983) with the kinetic scheme shown in Scheme III to provide the best fit of the observed pre-steady-state data. (As will be discussed in the next section, all of the rate constants in this scheme, except for hydride transfer from NADPH to H_2F, were determined independently.) The simulated curves shown in Figure 1 were determined with KINSIM

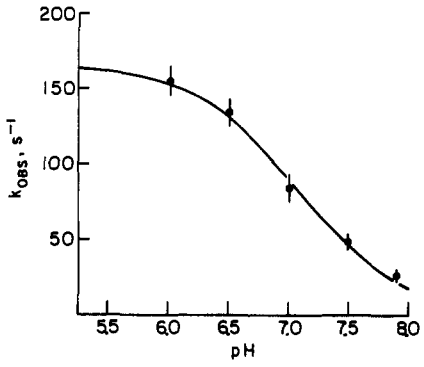

FIGURE 2: Observed rate constant for hydride transfer catalyzed by Val-113 DHFR as a function of pH. Final conditions are 10 μM DHFR, 112 μM H_2F, and 87 μM NADPH in MTEN buffer, 25 °C. The rate constant for hydride transfer is calculated by using KINSIM and Scheme III as described in the text. The solid line is fit to the equation $k_{obs} = k_{hyd}/(1 + K_a/[H^+])$, where $k_{hyd} = 165 \pm 5$ s^{-1} and $pK_a = 7.08 \pm 0.05$.

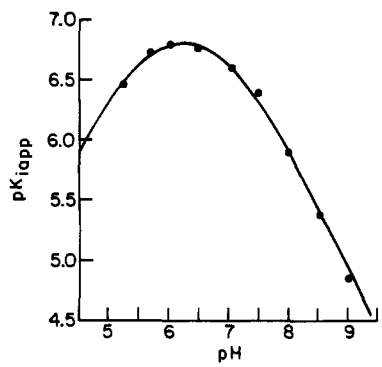

FIGURE 3: Variation with pH of the $pK_{i,app}$ ($-\log K_{i,app}$) for inhibition of V-113 DHFR by 2,4-diamino-6,7-dimethylpteridine. The theoretical curve is drawn according to eq 3, where $pK_i = 6.96$, $pK_A = 6.96$, and $pK_B = 5.56$.

Scheme IV: pH-Dependent Kinetic Scheme for Val-113 Dihydrofolate Reductase in MTEN Buffer, 25 °C[a]

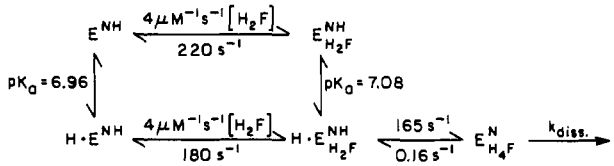

[a] N, NADP; NH, NADPH; H_2F, dihydrofolate; H_4F, tetrahydrofolate.

using ${}^{H}k_{hyd} = 155 \pm 10$ s^{-1} and ${}^{D}k_{hyd} = 49 \pm 5$ s^{-1}, which means that the intrinsic deuterium isotope effect is 3.2 ± 0.5, consistent with the value measured at high pH for Val-113 and for wild-type (see Table IV).

Like wild-type DHFR, the steady-state kinetics of Val-113 are pH dependent, which can be fit by a single pK_a with decreasing rate as the pH increases (Chen et al., 1985). To determine the intrinsic pK_a of the E·NH·H_2F ternary complex, we measured the pH dependence of the observed hydride-transfer rate constant as shown in Figure 2. The hydride-transfer rate constants were estimated by using KINSIM as described for Figure 1. When these data are fit to a single pK_a by using a nonlinear least-squares fitting program, the pH-independent rate constant for hydride transfer is calculated to be $k_{hyd} = 165 \pm 5$ s^{-1}, and the pK_a of the ternary complex is 7.08 ± 0.05. Thus, the rate of hydride transfer is slower than that for wild-type ($k_{hyd} = 950 \pm 50$ s^{-1}), and the pK_a is higher than that for wild-type ($pK_a = 6.5 \pm 0.1$) (Fierke et al., 1987a).

pH Dependence of DAM Inhibition. To determine the pK_a of the E·NH binary complex, the pH dependence of inhibition of Val-113 DHFR turnover by a folate substrate analogue, 2,4-diamino-6,7-dimethylpteridine (DAM), was measured. Analysis of the pH dependence of competitive inhibition will generally yield the correct pK_a value (Cleland, 1977). The variation of the observed $pK_{i,app}$ for inhibition of Val-113 DHFR by DAM as a function of pH yields the bell-shaped curve shown in Figure 3, which when fit to eq 3 for two pK_as

$$K_{i,app} = K_i\left(1 + \frac{H}{K_B}\right)\left(1 + \frac{K_A}{H}\right) \quad (3)$$

yields $pK_i = 6.96 \pm 0.06$, $pK_A = 6.96 \pm 0.07$, and $pK_B = 5.56 \pm 0.13$. The $pK_B = 5.56$ is due to protonation of the N-1 nitrogen of DAM, which has been directly determined to be $pK_a = 5.75 \pm 0.03$ and has been shown to decrease inhibitor binding to wild-type DHFR (Stone & Morrison, 1983). The pK_A value of 6.96 must reflect the pK_a of a group on the enzyme since DAM does not have a group with a pK_a value in this region. This pK_a agrees well with the pK_a of 7.08 measured for the pH dependence of the hydride-transfer rate and, similar to wild-type, is likely due to Asp-27 (Howell et al., 1986).

DISCUSSION

Summary of Overall Kinetic Scheme. From the data presented under Results it is possible to construct a complete kinetic scheme for Val-113-DHFR-catalyzed reduction of H_2F as shown in Scheme III. The heavy arrows indicate the kinetic pathway for steady-state turnover under saturating conditions. The association and dissociation rate constants for the formation of all binary complexes and the formation of the ternary complex, E·NH·H_4F, were measured directly as well as the dissociation rate constants from E·N·H_4F. Direct measurement of the association and dissociation rate constants for formation of the substrate ternary complex, E·NH·H_2F, is impossible, as this complex is reactive. Since folate is a poor substrate for *E. coli* DHFR (Stone & Morrison, 1986), it was used as a H_2F analogue to estimate the association and dissociation rate constants for binding NADPH to E·H_2F. The association and dissociation rate constants for binding H_2F to E·NH were assumed to be the same as binding to E, as observed for wild-type DHFR (Fierke et al., 1987a), which balances the equilibrium binding within the closed system. The enzyme-catalyzed rate constant for hydride transfer from NADPH to H_2F in the protonated ternary complex (H·E·NH·H_2F) is the observed hydride-transfer rate extrapolated to low pH, $k_{hyd} = 165$ s^{-1} (Figure 2). The rate constant for hydride transfer in the reverse direction (H_4F to NADP) was estimated to be 0.17 s^{-1} from the observed steady-state rate constant in this direction at pH 10 with saturating substrates. Hydride transfer is the main rate-limiting step under these conditions since it is rate-limiting in the forward direction at high pH (${}^{H}k_{cat}/{}^{D}k_{cat} \approx 3.0$) and the measured product (NADPH and H_2F) dissociation rate constants are fast.

The pH dependence of this reaction is illustrated in Scheme IV. A single pK_a of 7.08 is observed in the pre-steady-state, which is the pK_a for the E·NH·H_2F complex. An identical pK_a is measured for the E·NH binary complex from the pH dependence of competitive inhibition by DAM. In this study there is no evidence for slow (<300 s^{-1}) proton transfer between either enzyme and solvent or enzyme and H_2F.

A good test of the validity of Schemes III and IV is a comparison of the measured steady-state parameters with those predicted from this model as shown in Table IV. Steady-state kinetic parameters for the proposed scheme (Schemes III and IV) were determined by double-reciprocal plots of data sim-

ulated by using the computer program KINSIM (Barshop et al., 1983) at a variety of substrate concentrations and pHs and assuming that the binding rate constants are pH independent as observed for wild-type DHFR (Fierke et al., 1987a). The isotope effect data were simulated by using an intrinsic isotope effect on hydride transfer of 3 as measured for wild-type and other mutant DHFR proteins (Fierke et al., 1987a; Chen et al., 1987). The identical steady-state kinetic parameters can also be calculated from the steady-state kinetic expressions for this model described in the Appendix of Chen et al. (1987). Thus, Schemes III and IV can adequately predict all of the observed steady-state kinetic behavior, as shown in Table IV. In addition, the internal equilibrium constant, $K_{int} = 970$, can be scaled to the overall pH-independent equilibrium constant of 1.3×10^{11} M^{-1} (Fierke et al., 1987a) within experimental error, where $K_{ov} = K_{int}(1/K_a)(K_4/K_2) = (6.5 \pm 5) \times 10^{10}$ M^{-1} (Scheme V).

Scheme V

$$E + H \underset{K_a}{\rightleftharpoons} H\cdot E + NH + H_2F \underset{K_2}{\rightleftharpoons} H\cdot E\cdot NH\cdot H_2F \overset{K_{int}}{\rightleftharpoons}$$

$$E\cdot N\cdot H_4F \overset{K_4}{\rightleftharpoons} E + N + H_4F$$

The steady-state kinetic expressions for these schemes predict varying rate-limiting steps under a variety of conditions. At low pH under k_{cat} conditions there is no single rate-limiting step; hydride transfer, NADP dissociation, and H_4F dissociation from $E\cdot NH\cdot H_4F$ all contribute to the observed steady-state turnover. At high pH hydride transfer becomes solely rate-limiting, as evidenced by the large observed isotope effect. Under k_{cat}/K_M conditions at low pH both H_2F binding and hydride transfer contribute to the observed rate constant, while at high pH hydride transfer again becomes completely rate-limiting. The observed pK_as in both k_{cat} and k_{cat}/K_M are perturbed upward from the intrinsic pK_a of the ternary complex due to the nonequilibrium binding of H_2F for k_{cat}/K_M and the change in rate-limiting steps for k_{cat}.

Comparison of Wild-Type and Val-113 DHFRs. Thr-113 is a strictly conserved residue in the H_2F binding site that from the X-ray crystal structure (Bolin et al., 1982) interacts with the proton-donating residue, Asp-27 (Howell et al., 1986), via one hydrogen bond and with the 2-amino group of methotrexate (and by analogy, H_2F) indirectly through a hydrogen bond with a fixed water molecule. In the Val-113 mutant, the methyl group of valine replaces the hydroxyl group, causing the disruption of one or two hydrogen bonds.

In the study of mutant proteins it is necessary to assess the structural integrity of the mutant. Recent crystallographic studies indicate that point mutations are in general accommodated by very minor adjustments of the tertiary protein structure along with changes in the position of solvent molecules (Howell et al., 1986; Sprang et al., 1987; Alber et al., 1987). We have examined thermodynamic dissociation constants, kinetic binding constants, and the conformational states of DHFR to estimate the effect of the single amino acid change on structure. The mutation Thr-113 → Val has little or no effect on the binding of NADP but does slightly weaken the binding of NADPH by increasing the NADPH dissociation rate constant about 4-fold (Tables I–III). As illustrated in Scheme I, *E. coli* DHFR exists in two slowly interconverting conformational states, E_1 and E_2. The change of Thr-113 to Val produced little change in the relative E_1 and E_2 distributions, with no effect on the rate constant for conversion of E_2 to E_1. From these results, along with the similarity in the overall kinetic scheme to wild-type, we conclude that the Val-113 mutation has the same gross conformation as the wild-type, although the mutation does affect the nicotinamide binding pocket to a small extent, as well as the folate binding pocket. We cannot rule out local conformational changes of either the protein or the bound substrate.

The overall kinetic scheme of Val-113 is identical in form with wild-type, although many of the rate constants differ. Several key features of these schemes (Scheme III; Fierke et al., 1987a) are the following: (i) The rate constant for steady-state turnover at neutral pH is partially or completely limited by H_4F release. (ii) Dissociation of H_4F is fastest from the mixed ternary $E\cdot NH\cdot H_4F$ complex, so that the kinetic pathway for steady-state turnover at saturating substrate follows a specific, preferred pathway in which H_4F dissociation from DHFR occurs after NADPH replaces NADP; consequently, successive catalytic cycles are interlocked. (iii) The internal equilibrium constant for hydride transfer on the enzyme, K_{int}, is large [K_{int}(pH 7) = 380 (wild-type), 513 (V-113)], partially reflecting the favorable equilibrium constant for formation of H_4F and NADP in the overall equilibrium [K_{ov}(pH7) $\approx 10^4$].

Despite these similarities, the replacement of a hydroxyl group with a methyl group at position 113 affects the magnitude of many rate constants in the kinetic scheme. First, this mutation decreases the binding of substrates and inhibitors in the folate binding site by about 2.3 kcal/mol (Table III). This overall decrease in binding is due to both a 5–10-fold decrease in the association rate constant (0.9–1.4 kcal/mol) and a 9–25-fold increase in the dissociation rate constant (1.3–1.9 kcal/mol, see Tables I and II). These overall changes in free energy for removal of a hydroxyl group are larger than those of 0.5–1.5 kcal/mol observed by Fersht et al. (1985) for loss of a single hydrogen bond to an unchanged donor in the enzyme tyrosyl synthetase. It is likely that in this mutation (Thr-113 → Val) the apparent binding energy for interaction of OH with the substrate, ΔG_{app}, is not due solely to the incremental binding energy of a single hydrogen bond, ΔG_{bind} (Fersht, 1988). Additional factors that could contribute to the observed loss of binding energy include (i) small structural changes in the folate binding site, (ii) unfavorable steric interactions between the methyl group of Thr-113 and either bound ligand or nearby side chains, and (iii) movement of active-site water molecules.

Second, the Thr-113 to Val mutation affects the pK_a of the active-site Asp-27; it increases from a pK_a of 6.5 in the wild-type (already a perturbed pK_a) to 7.05 in the mutant, an increase in $\Delta\Delta G$ of 0.75 kcal/mol. There is no evidence that this mutation substantially decreases the rate constant for proton transfer. The crystal structure for the wild-type enzyme (Filman et al., 1982; Bolin et al., 1982) shows that Thr-113 forms a hydrogen bond with Asp-27, presumably in both the protonated and unprotonated forms. From the above results we conclude that in the hydrophobic environment of the active site of DHFR the hydrogen bond stabilizes the carboxylate to a larger extent than the acid, thus causing an increase in pK_a in the mutant. This conclusion is consistent with those of Fersht (1985, 1988) suggesting that hydrogen bonds to charged acceptors are stronger than those to uncharged acceptors. In addition, the kinetics of this mutation clearly illustrate that Thr-113 is not absolutely required in the pathway for protonation of Asp-27 from solvent (Chen et al., 1985).

Finally, the rate constant for hydride transfer from NADPH to H_2F in the $H\cdot E\cdot NH\cdot H_2F$ complex is decreased 6-fold (1.0 kcal/mol) in the Val-113 mutant compared to wild-type. The rate constant for hydride transfer from H_4F to NADP on the

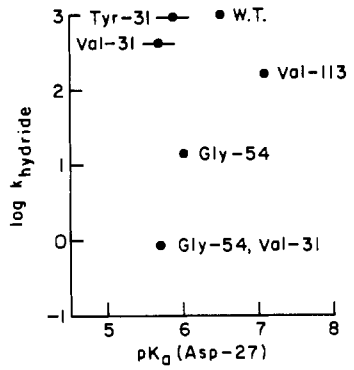

FIGURE 4: Plot of log k_{hyd} versus pK_a of Asp-27 for mutations in the folate binding site. k_{hyd} and the pK_a for Tyr-31, Val-31 (Taira et al., 1987a), wild-type (Fierke et al., 1987a), and Val-113 DHFRs were determined from pre-steady-state kinetics and for Gly-54 and [Gly-54, Val-31] DHFRs were determined from steady-state kinetics (Mayer et al., 1986; Mayer and Benkovic, unpublished results).

enzyme is also decreased 3.5-fold (0.7 kcal/mol), which means that the overall internal equilibrium constant is largely unaffected [1583 (wild-type) vs 971 (V-113)]. Owing to the difference in pK_as, at high pH the ratio between the observed forward rate constants for hydride transfer is smaller [k_{hyd}(pH 9) = 3 s^{-1} (wild-type) vs 1.8 s^{-1} (V-113)] and the observed internal equilibrium constant is more favorable for V-113 [K_{int}(pH 9) = 5 (wild-type) vs 11 (V-113)]. At neutral pH the increased pK_a of Asp-27 largely compensates for the decreased forward hydride-transfer rate constant. Thus, in this mutant the decrease in the rate constant for hydride transfer may be correlated with a decrease in the acidity of Asp-27. This phenomenon is not general in DHFR mutants; in a large number of mutants in the folate binding site there is no correlation between the rate constant for hydride transfer, k_{hyd}, and the pK_a of Asp-27 as illustrated in Figure 4. Alternatively, the decrease in the hydride-transfer rate constant (k_{hyd}) can be correlated with the decrease in binding in the folate binding sites (K_D) for a large number of mutants including V-113 (Benkovic et al., 1988).

From the complete kinetic schemes for wild-type and Val-113 DHFR it is possible to construct a reaction coordinate diagram for turnover at defined substrate concentrations. We have chosen to use substrate concentrations approximating those of the *E. coli* cell, namely, 1.0 mM NADPH, 1.5 mM NADP (Lilius et al., 1979), 0.3 μM H_2F and 13 μM H_4F (D. Duch, personal communication), and 0.1 M NaCl, pH 7.0, 25 °C. The two diagrams (Figure 5), aligned at the binary E·NADPH complex, clearly illustrate that under these conditions the Thr-113 → Val mutation causes two major effects: (i) the binding of H_2F and H_4F is decreased and (ii) the equilibrium constant for hydride transfer is unaffected, but the transition state is destabilized. Thus, two nonchemical steps are partially rate-limiting: H_2F binding and H_4F dissociation. Although under these conditions the overall reaction strongly favors H_4F formation (K_{eq} = 450), the assumed concentration of H_4F causes accumulation of E·NH·H_4F and E·N·H_4F during steady-state turnover.

Given the definition of the kinetic sequence, one can calculate the net velocity, v_{net}^f, for formation of NADP and H_4F as described by Segel (1975). The net velocity as a function of microscopic rate constants for the major pathway during steady-state turnover (Scheme VI) is shown in eq 4. We can then use the net velocity to calculate the catalytic efficiency of mutant and wild-type DHFRs. As defined by Albery and Knowles (1976), an efficient enzyme will mediate a high flux of substrate to product with a maximum catalytic flux defined

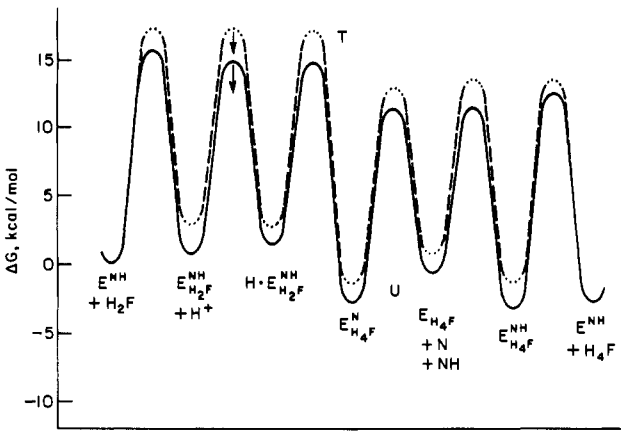

FIGURE 5: Gibbs free energy coordinate diagrams for *E. coli* wild-type (—) and Val-113 mutant (---) dihydrofolate reductase aligned at the substrate binary complex, E·NH, calculated for the following conditions: 1.0 mM NADPH, 1.5 mM NADP, 0.3 μM H_2F, 13 μM H_4F, and 0.1 M NaCl, pH 7.0, 25 °C. The designations T and U refer to transition state and uniform binding, respectively.

by the diffusion-limited rate constant for binding substrate to enzyme. Since the concentration of NADPH is so much larger than that of H_2F, we have chosen to calculate the theoretical maximum velocity, $v_{net}^0/[E]$, employing the measured association rate constant of 4×10^7 M^{-1} s^{-1} for H_2F binding to wild-type E·NH as a diffusion-controlled process (Penner & Frieden, 1987; Fierke et al., 1987a), so that under these conditions $v_{net}^0/[E]$ = 12 s^{-1}. [The maximum velocity would be affected by any mechanism, such as channeling, that changes the association rate constant (Young et al., 1985).] The efficiency, E_f, of an enzyme is calculated from the ratio of the observed net velocity to the theoretical maximum velocity.

Scheme VI

$$E^{NH} \underset{k_2}{\overset{k_1(H_2F)}{\rightleftharpoons}} E^{NH}_{H_2F} \underset{k_4}{\overset{k_3}{\rightleftharpoons}} E^{N}_{H_4F} \underset{k_6[N]}{\overset{k_5}{\rightleftharpoons}} E_{H_4F} \underset{k_8}{\overset{k_7[NH]}{\rightleftharpoons}} E^{NH}_{H_4F} \underset{k_{10}[H_4F]}{\overset{k_9}{\rightleftharpoons}} E^{NH}$$

$$v_{net}/[E] = (k_1[H_2F]k_3k_5k_7[NH]k_9 - k_2k_4k_6[N]k_8k_{10}[H_4F])/\{k_4k_9[(k_1[H_2F] + k_2) \times (k_6[N] + k_7[NH])] + k_3k_8[(k_1[H_2F] + k_{10}[H_4F])(k_5 + k_6[N])] + k_2k_{10}[H_4F][(k_7[NH] + k_8)(k_4 + k_5)] + k_5k_7[NH][k_3(k_1[H_2F] + k_{10}[H_4F]) + k_9(k_1[H_2F] + k_2 + k_3)] + k_6[N][k_4k_8(k_1[H_2F] + k_2 + k_{10}[H_4F])] + k_2k_{10}[H_4F](k_4 + k_8)] + k_1[H_4F]k_3k_9(k_5 + k_6[N] + k_7[NH])\} \quad (4)$$

The calculated efficiency for wild-type DHFR, 16% (Table V), is high, although less than that observed for triosephosphate isomerase, 60% (Albery & Knowles, 1976). In the absence of H_4F the efficiency of DHFR increases to 37%, and it is clear from an examination of Figure 5 that ground-state destabilization of E·NH·H_4F might represent a means for improving the efficiency. Although theoretically the efficiency of DHFR could be increased, all of the active-site mutations studied to date have decreased efficiency (Table V) due to an unfavorable compensation between an increased product dissociation rate constant, k_9, and a decreased rate constant for binding H_2F, k_1, or hydride transfer, k_3. For example, the decrease in efficiency in Val-113 DHFR is caused mainly by a 10-fold decrease in k_1. Consequently, the division of free energy change of the chemical reaction into the steps exhibited in Figure 5 is a satisfactory solution to the problem of catalyzing the given reactions under the presumed conditions. As dis-

Table V: Efficiency of DHFR Mutants: Physiological Conditions

enzyme	$v_{net}^f/[E]$ (s^{-1})	% efficiency[a]
wild-type	1.9[a]	16
Phe-31 → Tyr	1.2[b,c]	10
Thr-113 → Val	0.31[a]	2.6
Phe-31 → Val	0.27[b,c]	2.2
Leu-54 → Gly	0.030[b,d]	0.25
[Asp-27 → Ser, Thr-113 → Gly]	0.0026[b,e]	0.022
Asp-27 → Ser	9.2×10^{-4} [b,f]	0.008
Asp-27 → Asn	6.6×10^{-4} [b,f]	0.0055
Thr-113 → Glu	3.0×10^{-5} [b,e]	0.0003
[Leu-54 → Gly, Phe-31 → Val]	1.4×10^{-5} [b,d]	0.0001

[a] Calculated as described in the text for 0.3 μM H_2F, 13 μM H_4F, pH 7.0, 25 °C. [b] Calculated as $v_{net}^f/[E] = (k_{cat}^f/K_M^f)[H_2F]/(1 + [H_2F]/K_M^f + [H_4F]/K_M^r)$, where $K_M^r \approx 10K_M^f$. [c] Taken from Chen et al. (1987). [d] Taken from Mayer et al. (1986). [e] Taken from Howell et al. (1987). [f] Taken from Howell et al. (1986).

cussed elsewhere (Fierke et al., 1987b), the efficiency of wild-type DHFR could be further optimized to 0.8 by (i) destabilizing the intermediates $E^N_{H_4F}$ and $E^N_{H_2F}$ and the associated transition state by about 2.0, 3.0, and 1.8 kcal/mol, respectively, and (ii) stabilizing the transition state for hydride transfer by about 0.4 kcal/mol.

In terms of the evolution of catalytic behavior (Albery & Knowles, 1976), hypothetical improvements in enzyme efficiency may be achieved by three means: uniform binding in which the free energies of internal ground and transition states change equally; differential binding in which the free energies of the internal intermediates and their associated transition states vary relative to one another in a linear fashion; and fine tuning of the free energy of a specific transition state. The Thr-113 to Val DHFR mutation is manifest in both uniform free energy changes for the intermediates $E^N_{H_4F}$ and E_{H_4F} and the intervening transition state as well as a specific effect on the transition state in hydride transfer. Differential effects are exhibited by the remaining intermediates. Mutants of β-galactosidase (Hall et al., 1983) and tyrosyl-tRNA synthetase (Ho & Fersht, 1986) likewise show no clean separation of uniform, differential, or transition-state binding processes. It appears likely that strictly conserved active-site residues can be expected to manifest multiple effects on key ground and transition states, so that in an evolutionary sense all the energetic aspects of turnover may be sampled simultaneously. Consequently, when was this residue incorporated?

ACKNOWLEDGMENTS

We thank S. Singer for providing us with *E. coli* strain SF32 and R. J. Mayer for preparing the V-113 mutant as well as for helpful discussions. We especially thank K. A. Johnson for his many useful suggestions.

Registry No. H_2F, 4033-27-6; H_4F, 135-16-0; DHFR, 9002-03-3; MTX, 59-05-2; NADPH, 53-57-6; NADP, 53-59-8; DAM, 1425-63-4; L-Val, 72-18-4; L-Thr, 72-19-5.

REFERENCES

Alber, T., Dao-pin, S., Wilson, K., Wozniak, J. A., Cook, S. P., & Matthews, B. W. (1987) *Nature (London) 330*, 41–46.

Albery, W. J., & Knowles, J. R. (1976) *Biochemistry 15*, 5631–5640.

Baccanari, D. P., Averett, D., Briggs, C., & Burchall, J. (1977) *Biochemistry 16*, 3566–3572.

Barshop, B. A., Wrenn, R. F., & Frieden, C. (1983) *Anal. Biochem. 130*, 134–145.

Benkovic, S. J., Fierke, C. A., & Naylor, A. M. (1988) *Science (Washington, D.C.) 239*, 1105–1110.

Birdsall, B., Burgen, A. S. V., & Roberts, G. C. K. (1980) *Biochemistry 19*, 3723–3731.

Blakley, R. L. (1960) *Nature (London) 188*, 231–232.

Bolin, J. T., Filman, D. J., Matthews, D. A., Hamlin, R. C., & Kraut, J. (1982) *J. Biol. Chem. 257*, 13650–13662.

Brown, D. J., & Jacobsen, N. W. (1961) *J. Chem. Soc.*, 4413–4420.

Cayley, P. J., Dunn, S. M. J., & King, R. W. (1981) *Biochemistry 20*, 874–879.

Chen, J.-T., Mayer, R. J., Fierke, C. A., & Benkovic, S. J. (1985) *J. Cell. Biochem. 29*, 73–82.

Chen, J.-T., Taira, K., Tu, C.-P., & Benkovic, S. J. (1987) *Biochemistry 26*, 4093–4100.

Chin, J. (1983) *J. Am. Chem. Soc. 105*, 6502–6503.

Chothia, C., & Lesk, A. M. (1985) *J. Mol. Biol. 182*, 151–158.

Cleland, W. W. (1977) *Adv. Enzymol. Relat. Areas Mol. Biol. 45*, 273–387.

Curthoys, H. P., Scott, J. M., & Rabinowitz, S. C. (1972) *J. Biol. Chem. 247*, 1959–1964.

Dawson, R. M. C., Elliott, D. C., Elliott, W. H., & Jones, K. M. (1969) *Data for Biochemical Research*, Oxford University, Oxford, U.K.

Dunn, S. M. J., & King, R. W. (1980) *Biochemistry 19*, 766–773.

Dunn, S. M. J., Batchelor, J. G., & King, R. W. (1978) *Biochemistry 17*, 2356–2364.

Dyson, R. D., & Isenberg, I. (1971) *Biochemistry 10*, 3233–3241.

Ellis, K. J., & Morrison, J. F. (1982) *Methods Enzymol. 87*, 405–426.

Fersht, A. R. (1988) *Biochemistry 27*, 1577–1580.

Fersht, A. R., Shi, J.-P., Knill-Jones, J., Lowe, D. M., Wilkinson, A. J., Blow, D. M., Brick, P., Carter, P., Waye, M. M. Y., & Winter, G. (1985) *Nature (London) 314*, 235–238.

Fierke, C. A., Johnson, K. A., & Benkovic, S. J. (1987a) *Biochemistry 26*, 4085–4092.

Fierke, C. A., Kuchta, R. D., Johnson, K. A., & Benkovic, S. J. (1987b) *Cold Spring Harbor Symp. Quant. Biol. 52*, 631–638.

Filman, D. J., Bolin, J. T., Matthews, D. A., & Kraut, J. (1982) *J. Biol. Chem. 257*, 13663–13672.

Hall, B. G., Murray, M., Osborne, S., & Sinott, M. L. (1983) *J. Chem. Soc., Perkin Trans 2*, 1595–1598.

Ho, C. K., & Fersht, A. R. (1986) *Biochemistry 25*, 1891–1897.

Howell, E. E., Villafranca, J. E., Warren, M. S., Oakley, S. J., & Kraut, J. (1986) *Science (Washington, D.C.) 231*, 1123–1128.

Howell, E. E., Warren, M. S., Booth, C. L. J., Villafranca, J. E., & Kraut, J. (1987) *Biochemistry 26*, 8591–8598.

Johnson, K. A. (1986) *Methods Enzymol. 134*, 677–705.

Kallen, R. G., & Jencks, W. P. (1966) *J. Biol. Chem. 241*, 5845–5850.

Lakowicz, J. R. (1983) *Principles of Fluorescence Spectroscopy*, Plenum, New York.

Lilius, E.-M., Multanen, V.-M., & Toivonen, V. (1979) *Anal. Biochem. 99*, 22–27.

Mathews, C. K., & Huennekens, F. M. (1963) *J. Biol. Chem. 235*, 3304–3308.

Matthews, D. A., Bolin, J. T., Burridge, J. M., Filman, D. J., Volz, K. W., Kaufman, B. T., Beddell, C. R., Champness, J. N., Stammer, D. K., & Kraut, J. (1985) *J. Biol. Chem. 260*, 381–391.

Mayer, R. J., Chen, J.-T., Taira, K., Fierke, C. A., & Benkovic, S. J. (1986) *Proc. Natl. Acad. Sci. U.S.A. 83*, 7718–7720.

Penner, M. H., & Frieden, C. (1985) *J. Biol. Chem. 260*, 5366-5369.
P-L Biochemicals (1961) Circular OR-18, Milwaukee, WI.
Rabinowitz, J. C. (1960) *Enzymes, 2nd Ed. 2*, 185-252.
Raines, R. (1986) Doctoral Dissertation, Harvard University, Cambridge, MA.
Roth, B., & Strelitz, J. Z. (1969) *J. Org. Chem. 34*, 821-836.
Seeger, D. R., Cosulich, D. B., Smith, J. M., & Hultquist, M. E. (1949) *J. Am. Chem. Soc. 71*, 1753-1758.
Segel, I. H. (1975) in *Enzyme Kinetics, Behavior and Analysis of Rapid Equilibrium and Steady-State Enzyme Systems*, p 109, Wiley-Interscience, New York.
Singer, S., Ferone, R., Walton, L., & Elwell, L. (1985) *J. Bacteriol. 164*, 470-472.
Smith, D. R., & Calvo, J. M. (1980) *Nucleic Acids Res. 8*, 2255-2274.
Smith, G. K., Benkovic, P. A., & Benkovic, S. J. (1981) *Biochemistry 20*, 4034-4036.
Smith, M. (1985) *Annu. Rev. Genet. 19*, 423-462.
Sprang, S., Standing, T., Fletterick, R. J., Stroud, R. M., Finer-Moore, J., Xuang, N.-H., Hamlin, R., Rutter, W. J., & Craik, C. S. (1987) *Science (Washington, D.C.) 237*, 905-909.
Stone, S. R., & Morrison, J. F. (1982) *Biochemistry 21*, 3757-3765.
Stone, S. R., & Morrison, J. F. (1983) *Biochim. Biophys. Acta 745*, 247-258.
Stone, S. R., & Morrison, J. F. (1984) *Biochemistry 23*, 2753-2758.
Stone, S. R., & Morrison, J. F. (1986) *Biochim. Biophys. Acta 869*, 275-285.
Strauss, D., Kawashima, R. E., Knowles, J. R., & Gilbert, W. (1985) *Proc. Natl. Acad. Sci. U.S.A. 82*, 2272-2276.
Taira, K., & Benkovic, S. J. (1988) *J. Med. Chem. 31*, 129-137.
Taira, K., Chen, J.-T., Mayer, R. J., & Benkovic, S. J. (1987a) *Bull. Chem. Soc. Jpn. 60*, 3017-3027.
Taira, K., Fierke, C. A., Chen, J.-T., Johnson, K. A., & Benkovic, S. J. (1987b) *Trends Biochem. Sci. (Pers. Ed.) 12*, 275-278.
Velick, S. F. (1958) *J. Biol. Chem. 233*, 1455-1467.
Villafranca, J. E., Howell, E. E., Voet, D. H., Strobel, M. S., Ogden, R. C., Abelson, J. N., & Kraut, J. (1983) *Science (Washington, D.C.) 222*, 782-788.
Villafranca, J. E., Howell, E. E., Oatley, S. J., Xuong, N., & Kraut, J. (1987) *Biochemistry 26*, 2182-2189.
Viola, R. E., Cook, P. F., & Cleland, W. W. (1979) *Anal. Biochem. 96*, 334-340.
Williams, J. W., Morrison, J. F., & Duggleby, R. G. (1979) *Biochemistry, 18*, 2567-2573.
Young, M., Wasserman, G., Benkovic, P., & Benkovic, S. (1985) *Proceedings of the Second Workshop on Folyl and Antifolyl Polyglutamates* (Goldman, I. D., Ed.) p 76, Praeger, New York.

Mechanism of Ketol Acid Reductoisomerase—Steady-State Analysis and Metal Ion Requirement†

Srinivas K. Chunduru, Gregory T. Mrachko, and K. C. Calvo*
Department of Chemistry, University of Akron, Akron, Ohio 44325
Received June 6, 1988; Revised Manuscript Received August 11, 1988

ABSTRACT: Ketol acid reductoisomerase is an enzyme of the branched-chain amino acid biosynthetic pathway. It catalyzes two separate reactions: an acetoin rearrangement and a reduction. This paper reports on the purification of the enzyme from a recombinant *Escherichia coli* and on the steady-state kinetics of the enzyme. The kinetics of the reaction were determined for the forward and reverse reaction by using the appropriate chiral substrates. At saturating metal ion concentrations the mechanism follows an ordered pathway where NADPH binds before acetolactate. The product of the rearrangement of acetolactate, 3-hydroxy-3-methyl-2-oxobutyrate, is shown to be kinetically competent as an intermediate in the enzyme-catalyzed reaction. Starting with acetolactate, Mg^{2+} is the only divalent metal ion that will support enzyme catalysis. For the reduction of 3-hydroxy-3-methyl-2-oxobutyrate, Mn^{2+} is catalytically active. Product and dead-end inhibition studies indicate that the binding of metal ion and NADPH occurs randomly. In the forward reaction direction, the deuterium kinetic isotope effect on V/K is 1.07 when acetolactate is the substrate and 1.39 when 3-hydroxy-3-methyl-2-oxobutyrate is the substrate.

The enzyme acetohydroxy acid reductoisomerase (2,3-dihydroxyisovalerate:$NADP^+$ oxidoreductase; EC 1.1.1.86) is found in the branched-chain amino acid biosynthetic pathway. It catalyzes the reaction indicated in eq 1. The two natural substrates for the enzyme differ in the identity of the R group that undergoes migration. In compound I, when R is methyl, biosynthesis proceeds to ultimately produce either valine or leucine. For the compound where R is ethyl, the ultimate

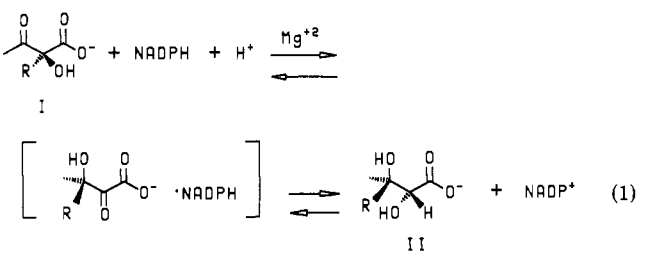

I II (1)

product is isoleucine. The enzyme reaction is unique in that an intramolecular alkyl transfer occurs without the intervention of cobalamin or any other organic cofactor. The enzyme

† Acknowledgment is made to the donors of the Petroleum Research Fund, administered by the American Chemical Society, for the support of this research.

0006-2960/89/0428-0486$01.50/0